First-principles calculations and tight-binding molecular dynamics simulations of the palladium-hydrogen system

A. Shabaev and D. A. Papaconstantopoulos
George Mason University, Fairfax, Virginia 22030, USA

M. J. Mehl and N. Bernstein
Naval Research Laboratory, Washington, DC 20375, USA

(Received 4 February 2010; revised manuscript received 19 April 2010; published 10 May 2010)

We present a study of palladium-hydrogen system by the linearized augmented plane-wave (LAPW) and Naval Research Laboratory (NRL) tight-binding (TB) methods. We constructed a TB Hamiltonian by fitting to first-principles LAPW data for the electronic energies of a large range of palladium and palladium hydride structures differing in symmetry and compositions as a function of volume. This TB Hamiltonian was then used to calculate phonon frequencies and elastic constants. Our calculations show good agreement with experiments and demonstrate the efficiency of the NRL-TB scheme. In addition, we performed tight-binding molecular dynamics simulations to calculate the density of states, mean-squared displacement, and the formation energy as a function of hydrogen content. We found a relative dip in the lattice energy of structures near the experimental limit of hydrogen content. We calculated the nearest hydrogen-hydrogen distance for various compositions of palladium hydride and confirmed the Switendick criterion.

DOI: 10.1103/PhysRevB.81.184103 PACS number(s): 71.15.Nc, 71.15.Pd

I. INTRODUCTION

Palladium has been known as an excellent metallic absorber of hydrogen for more than a century.[1] The ability to take up large volumes of hydrogen makes palladium efficient and safe storage of hydrogen and its isotopes. Considerable progress has been made in an investigation of structural, thermodynamic, and kinetic characteristics of this system.[2–5] Despite substantial development many important questions are not yet answered. The details of electronic energy states and the mechanism of hydrogen diffusion remain not fully understood. Of particular interest is the high solubility and mobility of the hydrogen in the face-centered-cubic (fcc) lattice of palladium, where the hydrogen atoms occupy octahedral sites.

A comprehensive model of the palladium-hydrogen system requires a description of the electronic structure and the bonding between the atoms. A range of methods has been used for electronic energy calculations in the palladium-hydrogen system varying from first-principles calculations[6,7] to pseudopotential methods[8] and other microscopic or semiempirical models.[9,10] The first-principles calculations are constrained to relatively small number of atoms and therefore are mostly limited to the calculations of stoichiometric compositions. Although the semiempirical microscopic models are better suited to treat large systems but they may not reveal essential details of the electronic structure. At an early stage, the tight-binding (TB) method in conjunction with the coherent-potential approximation was applied for calculating the band structure and density of states (DOS) in the palladium-hydrogen system including nonstoichiometric compositions.[11] The advantage of the TB method is efficiency in the calculations of large systems combined with the substantial level of the electronic spectrum details which can be handled by these calculations.

Recently the NRL-TB method has been developed to provide transferability between different structures and capability of calculating total energies.[12] In this method the parameters of the Slater-Koster Hamiltonian[13] are fit to reproduce a first-principles database of not only the band structures but also the total energies for several crystal structures differing in volume or symmetry.[14,15] In this paper we present the results of TB calculations for palladium hydride with a static atomic distribution and with molecular dynamics (MD) simulations of atomic motion for a wide range of temperatures, from 0 to 400 K. We apply static and dynamic methods to calculate the structural and electronic properties of palladium hydrogen including electron energies, elastic constants, phonon frequencies, mean-squared displacements, and formation energies as a function of hydrogen content.

II. FITTING TIGHT-BINDING PARAMETERS TO LAPW DATA

The NRL-TB method is based on fitting the on-site terms, the two-center Hamiltonian and the overlap parameters to the electronic eigenvalues and total energies provided by first-principles calculations. We have obtained the set of the TB parameters by fitting the total energy and the energy bands provided by our linearized augmented plane-wave (LAPW) calculations for a static distribution of atoms located at fixed lattice coordinates. We have carried out LAPW calculations for a large range of palladium and palladium hydride structures differing in symmetry and compositions. These structures included the palladium lattice of various symmetries, the simple-cubic hydrogen lattice, $L1_2$ lattice of Pd_3H and PdH_3, lattices with the five-atom supercell of Pd_4H, and with the seven-atom supercell of Pd_4H_3. Overall, we have calculated the energy for a total of 85 structures and volumes. Table I shows a wide range of compositions and structures with equilibrium lattice parameters found for each structure which formed a database that was the input to the tight-

TABLE I. Crystal structures used for fitting TB parameters.

Composition	Lattice	Equilibrium lattice constant (Å)
Pd	Body-centered cubic	5.79
Pd	Face-centered cubic	7.27
Pd	Simple cubic	4.805
PdH	NaCl	7.63
PdH	CsCl	4.935
PdH_2	CaF_2	8.29
Pd_4H	NaCl five-atom supercell	7.375
Pd_4H_3	NaCl seven-atom supercell	7.565
Pd_3H	$L1_2$	6.98
PdH_3	$L1_2$	5.425
H	Simple cubic	2.725

binding calculations. We fitted each structure for a wide range of the primitive cell volumes.

We have constructed a nonorthogonal two-center TB Hamiltonian using the s, p, d orbitals for palladium atoms and s, p orbitals for the hydrogen atoms by fitting the LAPW results for the total energy and the band structures. For atom i, the on-site TB parameters are defined as

$$h_{il} = a_l + b_l\rho_i^{2/3} + c_l\rho_i^{4/3} + d_l\rho_i^2, \quad (1)$$

where coefficients a_l, b_l, c_l, and d_l ($l=s$, p, or d) are the fitting parameters and the atom density ρ_i has the form

$$\rho_i = \sum_j \exp(-\lambda^2 R_{ij}) F(R_{ij}), \quad (2)$$

where the sum is over all atoms j within a range R_c of atom i, λ is a fitting parameter, and $F(R_{ij})$ is a cutoff function. In the two-center approximation, the hopping integrals depend only on the angular momentum dependence of the orbitals, $ll'u$ ($ss\sigma$, $sp\sigma$, $pp\sigma$, $pp\pi$, $sd\sigma$, $pd\sigma$, $dd\sigma$, $dd\pi$, and $dd\delta$) and the distance between the atoms. The s and p orbitals of hydrogen can only form ($ss\sigma$, $sp\sigma$, $pp\sigma$, and $pp\pi$) hopping integrals between each other and ($sd\sigma$ and $pd\sigma$) in addition for hopping between hydrogen and palladium. The hopping parameters for both the Hamiltonian and overlap matrices have the form

$$H_{ll'u}(R) = (e_{ll'u} + f_{ll'u}R + g_{ll'u}R^2)\exp(-q_{ll'u}^2 R) F(R), \quad (3)$$

where R is the separation between the atoms and ($e_{ll'u}$, $f_{ll'u}$, $g_{ll'u}$, and $q_{ll'u}$) are the fitting parameters. The overlap parameters have a form similar to the hopping parameters in Eq. (3). The values of the parameters are shown in the Appendix. This form of the TB parameters allows transferability to different crystal structures and atomic configurations.

The LAPW results for the formation energy are reproduced by the TB calculations with an accuracy up to 1 mRy and also shows the sodium chloride structure to be the ground state. This TB Hamiltonian also reproduces very well the energy bands and density of states of pure Pd and of the sodium chloride structure of PdH. Figure 1 shows how the

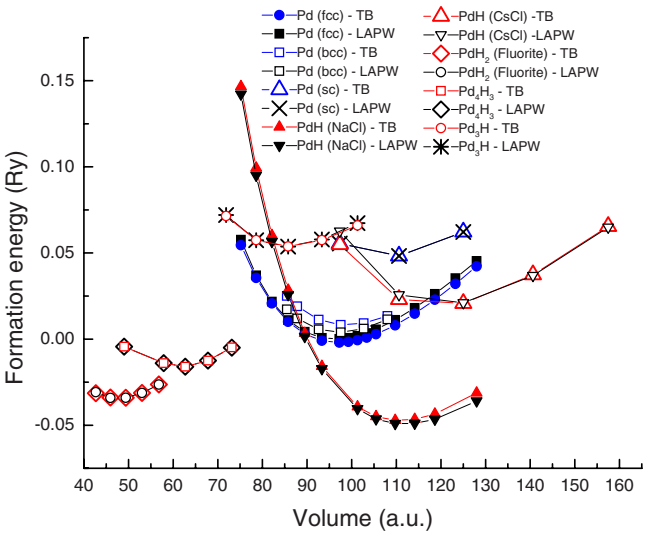

FIG. 1. (Color online) Total energy of various palladium and palladium hydride structures.

total energy is reproduced for some of the structures and volumes used for the fit. Each structure has its own minimum of the total energy. The minimum of the fcc structure, as expected, is the lowest one among the palladium structures. The total energy of the sodium chloride structure of palladium hydride compound is even lower. This structure reaches its minimum at a lattice constant of 4.04 Å which is larger than 3.85 Å the lattice constant of the lowest energy palladium structure fcc.[16] The larger lattice constant is in agreement with the experimentally observed expansion of the palladium lattice at higher concentrations of hydrogen.[5,17] The lattice constant linearly increases with the concentration of hydrogen in PdH_x and extrapolates to 4.09 Å for $x=1$.[18]

III. TIGHT-BINDING CALCULATIONS

The NRL-TB method is highly adapted and very efficient for calculations where the positions of atoms and distance between vary. We can calculate the energy of any structure with the same set of the parameters in a relatively wide range of interatomic distances.[14] The transferability of our TB parameters is tested by applying them to calculations of elastic constants, phonon frequencies, the coefficient of thermal expansion, and the vacancy formation energies. We have performed such calculations for the fcc structure of palladium[16] and the NaCl structure of palladium hydride at the equilibrium lattice constants.

A. Phonon frequencies

Phonon frequencies are obtained from the derivatives of the energy with respect to the displacement of the atoms from their equilibrium lattice positions. In the harmonic approximation, the potential energy as a function of the displacement and the energy variation can be written in the form[19]

TABLE II. Acoustic phonon frequencies of palladium deuteride (in terahertz).

Coordinates	Symmetry	Polarization	NRL-TB (PdD)	Experiment ($PdD_{0.63}$) (Ref. 21)
$(0,0,8)\ \frac{\pi}{4a}$	X_3	Longitudinal	6.07	5.5
	X_5	Transverse	3.47	4.0
$(4,4,4)\ \frac{\pi}{4a}$	L_2	Longitudinal	9.25	6.0
	L_3	Transverse	3.02	2.5

$$P_{\text{harm}} = \frac{1}{2} \sum_{\mathbf{R},\mathbf{R}',\alpha,\beta} \mathbf{u}^{\alpha}(\mathbf{R})\, \boldsymbol{\eta}^{\alpha\beta}(\mathbf{R}-\mathbf{R}')\mathbf{u}^{\beta}(\mathbf{R}'), \qquad (4)$$

where $\mathbf{u}^{\alpha}$ is the deviation from equilibrium of atom α on unit cell associated with lattice vector $\mathbf{R}$ and $\boldsymbol{\eta}^{\alpha\beta}(\mathbf{R}-\mathbf{R}')$ is the force-constant matrix. The number of independent force constants depends on a symmetry of a phonon mode. We have found the phonon frequencies by the frozen phonon method[19] where a unit cell is commensurate with the wave vector of the phonon and the displacements of atoms are chosen according to the polarization and the phase of the phonon mode. For the acoustic modes in the fcc palladium structure with a lattice constant of $a=3.847$ Å, our calculations[16] give very good agreement with experiment.[20] The acoustic frequencies in PdH are expected to be almost independent on the mass of the hydrogen isotope because the unit-cell center of mass oscillates with the acoustic modes and hence the frequency mostly depends on the mass of the heavy palladium atoms in the cell. According to experiment,[21] the acoustic frequencies are slightly lower in palladium deuteride than in pure palladium indicating that the presence of hydrogen isotope affects the frequencies by altering the interactions between the atoms and therefore the forces acting on these atoms. We calculated the acoustic phonon frequencies for the stoichiometric composition palladium deuteride. The results are shown in Table II. With the exception of the X_5 mode, the calculated frequencies are higher than the experimental values for $PdD_{0.63}$. At this time, we cannot definitively conclude if our results point to a nonmonotonic behavior of the acoustic frequencies with the hydrogen/deuterium content since the phonon frequencies have not been included into the LAPW database for the TB fit.

Another reason for the discrepancies in phonon frequencies is the substantial anharmonicity of the potential energy of hydrogen isotopes in palladium hydride. The effect of this anharmonicity was studied by Klein and Cohen[22] for the optical modes. In addition to the acoustic modes, there are three optical branches in palladium hydride. We have computed the optical phonon frequencies using the total-energy results obtained from the TB calculations. The results are shown in Table III. A relatively poor agreement with the experimental values is not surprising since for the fit of the TB parameters we have included the total energy calculated with the LAPW only at the Γ point. In any case, in the harmonic approximation, a satisfactory agreement with experiment is not expected for the frequencies obtained even with the LAPW total energies.[22] To evaluate the impact of this problem we have calculated the phonon frequencies with the LAPW total energies using the harmonic approximation.

The LAPW calculations have been performed for the stoichiometric composition ($x=1$) and for nonstoichiometric compositions with $x=0.63$. For the latter, we used the virtual-crystal approximation. We have calculated the total energy at the Γ and L points of the Brillouin zone. At the Γ point, the wave number of phonon mode is zero and therefore all atoms of the same kind oscillate in phase. The unit cell consists of one palladium and one hydrogen atoms which represent the dynamics of the entire lattice. The displacement of the hydrogen isotope is much larger than the displacement of the palladium atom since the center of mass of the unit cell is fixed in an optical mode and therefore the ratio of the atomic displacements is inversely proportional to the ratio of their masses. At the L point, two nearest hydrogen atoms oscillate with the opposite phases and therefore the unit cell should include two hydrogen and two palladium atoms to represent the displacements of the phonon mode.

The force constants are calculated by fitting the deviation of the total energy with displacement to the parabolic trend in Eq. (4) where all atoms in the sum belong to the unit cell used for the LAPW calculations. The $\boldsymbol{\eta}^{\alpha\beta}$ matrix is reduced

TABLE III. Optical phonon frequency of palladium deuteride PdD_x.

Symmetry	x	Lattice constant (Å)	Frequency (THz)		
			NRL-TB	LAPW	Experiment (Ref. 21)
Γ	1.00	4.02	8.70	7.59	
Γ	1.00	4.075	4.85	5.08	
L_3	1.00	4.02	9.12	4.34	
Γ	0.63	4.02		13.43	9.00
L_3	0.63	4.02		15.14	9.25

to a single constant η at the Γ point. At the L point, there are two force constants which correspond to the transverse and longitudinal oscillation modes. In both cases, the deviation of the total energy is fit to $\eta u^2/2$, where u is the relative displacement of either the hydrogen isotope and the palladium atom, for the Γ point, or two hydrogen isotopes, for the L point. Table III shows frequencies calculated as $(\eta/\mu)^{1/2}$, where μ is the reduced mass of two atoms: $\mu=m_{\mathrm{H}}m_{\mathrm{Pd}}/(m_{\mathrm{H}}+m_{\mathrm{Pd}})$ (Γ point) or $\mu=0.5m_{\mathrm{H}}$ (L point). The hydrogen mass should be replaced with the mass of deuterium for comparison with the experimental data.[21]

The frequencies are shown for two concentrations of deuterium: $x=0.63$ and $x=1.00$. The lattice constant varies with the deuterium content. The $x=0.63$ composition is calculated for the experimental lattice constant 4.02 Å and the $x=1.00$ composition is calculated for two values of the lattice constant 4.02 Å and the larger lattice constant of 4.075 Å which is near expected for $x=1.0$ from the experimental trend.[18] We have found that the frequency increases with a decrease in the lattice constant. Our calculations with the virtual-crystal approximation show that, the frequency changes with the composition even stronger than it is predicted by the calculations where the composition is fixed and the lattice constant is altered to simulate the variations in composition. Even for the fixed composition, the frequencies are more sensitive to the size of the lattice constant than it is expected from the calculations with the anharmonicity included into the potential which increases with the size of the lattice constant.[22] Despite the quantitative differences, our results are in qualitative agreement with Ref. 22 pointing to the softening of the frequencies of the optical phonon. Unlike the optical phonons, the acoustic branches do not vary substantially with the hydrogen isotope content. At the L point, the maximum acoustic frequency decreases from 6.9 THz in pure palladium to 6.0 THz in $PdD_{0.63}$.[21] The reduction in the frequency gap between the optical and acoustic modes indicates that the interaction between the hydrogen isotope and palladium sublattices weakens with an increase in hydrogen isotope concentration. The potential seen by a hydrogen isotope near its equilibrium position flattens with an increase in the hydrogen isotope concentration. This potential is likely formed by the palladium neighbors of the hydrogen isotope. Evidently the forces exerted on hydrogen atoms by the palladium lattice weaken as the interactions between palladium atoms experience relatively small variations. Above the limit in the hydrogen/deuterium content in palladium, the motion of hydrogen atoms become more independent of the palladium lattice. Each hydrogen atom can change its position with less energy penalty leading to instability of hydrogen distribution above the solubility limit. We found an additional demonstration of the dominating role of the interaction between hydrogen atoms and palladium neighbors as well as signs of structural instability in our tight-binding molecular dynamics (TBMD) study of vacancy formation energies we present below.

B. Elastic constants

The calculations of the elastic constants serve as a sensitive test for the TB parameters because the calculations depend on small differences between the equilibrium energies and the energy with the strain. We have shown that the TB calculations reproduce the elastic constants of palladium with ample accuracy.[16] We have also obtained the elastic constants for the palladium hydride and compared them with both the LAPW and experimental data. For the stoichiometric PdH structure, we have calculated the tetragonal shear modulus $(C_{11}-C_{12})/2$ for the orthorhombic strain and the trigonal shear modulus C_{44} for the monoclinic strain. The nonzero components of the strain tensor are $e_1=-e_2=\xi$, $e_3=\xi^2/(1-\xi^2)$ for the orthorhombic strain and $e_6=\xi$, $e_3=\xi^2/(4-\xi^2)$ for the monoclinic strain. The deviations of the total energy with the strain can be written as $V(C_{11}-C_{12})\xi^2$ and $VC_{44}\xi^2/2$, where V is the volume of undistorted lattice. The TB calculations provide the total energy and the pressure for various volumes near the minimum of the PdH structure (see Fig. 1). Using the TB results, we have calculated the bulk modulus as $B=V\cdot\partial^2E/\partial V^2=V\cdot\Delta P/\Delta V$, where ΔP and ΔV are the changes in the pressure and volume. Table IV shows the elastic-constant results of the TB calculations in comparison with the experimental data[23] for palladium hydride ($PdH_{0.66}$) with a hydrogen concentration of 66%.

TABLE IV. Elastic constants for palladium hydride (in gigapascal).

	NRL-TB	LAPW	Experiment (Ref. 23)
$\frac{1}{2}(C_{11}-C_{12})$	35.55	23.5	32.78
C_{44}	79.38	58	69.05
B	225.69	217	183.32

C. Molecular dynamics simulations

Using the NRL-TB parameters we performed MD simulations[24] for a supercell of 128 atoms for PdH shown in Fig. 2. The supercell is obtained by repeating the primitive cell four times along each of the primitive lattice directions.

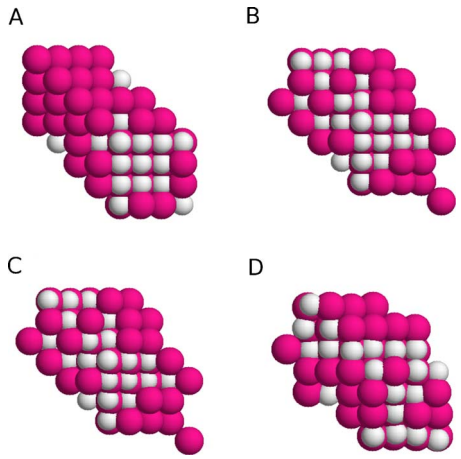

FIG. 2. (Color online) Evolution of palladium hydride supercell consisting of 128 atoms: A—initial fcc structure at $T=400$ K; B—4 fs elapsed time at $T=391$ K; C—16 fs elapsed time at $T=240$ K; D—570 fs elapsed time at $T=200$ K.

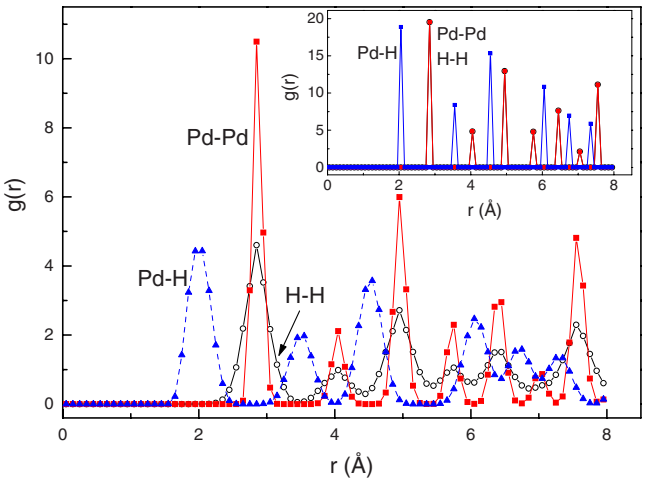

FIG. 3. (Color online) Radial-distribution function for Pd-Pd (red squares), H-H (black open circles), and Pd-H (blue triangles) correlations for equilibrium distribution at $T=200$ K [see Fig. 2(D)]. Inset: radial-distribution function for initial positions in TBMD simulations [see Fig. 2(A)].

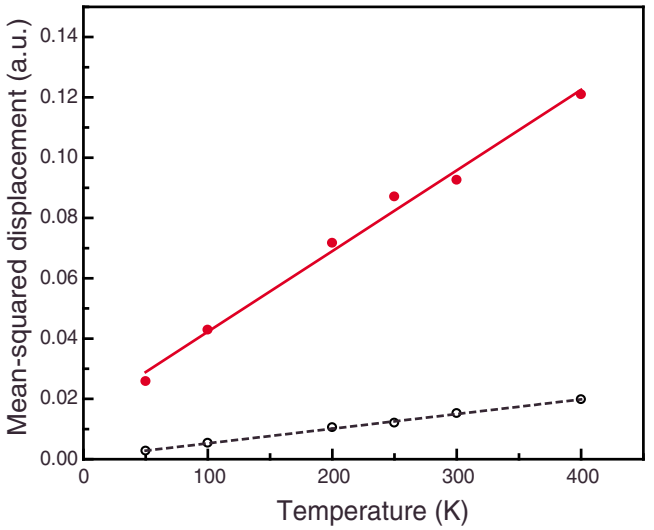

FIG. 4. (Color online) Mean-squared displacement for palladium (blue open) and hydrogen (red closed) atoms in PdH: calculated data (symbols) and fit (lines).

The simulations were performed for 3000 steps with a time step of 1 fs. Initially, the atoms are placed on the fcc lattice with random velocities with a Boltzmann distribution function for a temperature of $2T$. Very quickly in approximately 70 fs (35 steps), the atomic motion slows down and to the average velocities corresponding to the equilibrium at temperature T. The fluctuations are reduced to the normal equilibrium scale approximately in a picosecond time range. Figure 3 shows the radial-distribution function for the equilibrium distribution of atoms at $T=200$ K corresponding to a supercell in Fig. 2(D). The peaks correspond to the positions where the potential energy of atoms reaches its minimum (see the inset of Fig. 3). The initial distribution functions overlap for the hydrogen and palladium. For the equilibrium distribution at finite temperature, the radial-distribution functions are broadened due to atomic vibration. The equilibrium distribution is substantially more broadened for the hydrogen atoms because of their light mass.

We have performed the TBMD simulations for various temperatures from 50 to 400 K. We used the TBMD method to investigate the anharmonicity of the lattice energy. Additional information about the anharmonicity can be deduced from the calculations of the coefficient of thermal expansion and the mean-squared displacement. To evaluate qualitatively the anharmonicity we consider the following simple equation for the change in the energy with u, the displacement of an atom from its equilibrium position:

$$P(u) = \frac{1}{2}\eta u^2 - \frac{1}{3}\gamma u^3 + \frac{1}{4}\delta u^4. \quad (5)$$

The first term is the harmonic part [see Eq. (4)], and the second and the third terms are responsible for the thermal-expansion coefficient, α_L and the mean-squared displacements of palladium and hydrogen atoms.

D. Thermal-expansion coefficient

Using the TBMD simulation results for palladium hydride, we calculate the energy per unit volume or the pressure in the lattice for various temperatures and determine the thermal-expansion coefficient from $dP/dT=3\alpha_L B$, where B is the bulk modulus. The pressure changes linearly with the temperature within the entire range of our calculations with the slope of the linear fit 11.35 MPa/K. For the theoretical and experimental values of the bulk modulus of 225.69 and 183.32 GPa, we find $\alpha_L=1.7\times10^{-5}$ K^{-1} and 2×10^{-5} K^{-1} which are approximately two times larger than the thermal-expansion coefficient of pure palladium.[25]

E. Mean-squared displacement

For the stoichiometric palladium hydride, we have also determined the atomic mean-squared displacement of the Pd and H atoms for various temperatures between 50 and 400 K using the atomic positions recorded in the process of the MD simulation (see Fig. 4). First, we recorded the instantaneous positions $\mathbf{r}_j(n)$ of 128 atoms j at each simulation step n for the substantially large number of steps N in the range from $n=n_0$ to $n=n_0+N$. Next, we calculated the statistical mean-squared displacement by averaging the deviation of atomic positions squared over the snapshots recorded: $\langle u_j^2\rangle = \Sigma_{n=n_0}^{n_0+N}[\mathbf{r}_j(n)-\mathbf{r}_j(n_0)]^2/N$. Finally, we averaged the mean-squared displacements for each atom over all atoms of the same kind: hydrogen isotope $\langle u_{\mathrm{H}}^2\rangle=\Sigma_{j\in\mathrm{H}}\langle u_j^2\rangle/64$ or palladium $\langle u_{\mathrm{Pd}}^2\rangle=\Sigma_{j\in\mathrm{Pd}}\langle u_j^2\rangle/64$. In the range of relatively low temperatures, the mean-squared displacement changes linearly with the temperature. In this range, the palladium mean-squared displacements in PdH are almost identical to pure palladium measured experimentally[26] and calculated by the TBMD method.[16] The mean-squared displacement of the hydrogen atoms is varying from 0.025 a.u. at 50 K up to 0.12 a.u. at 400 K, which is close to the experimental value of

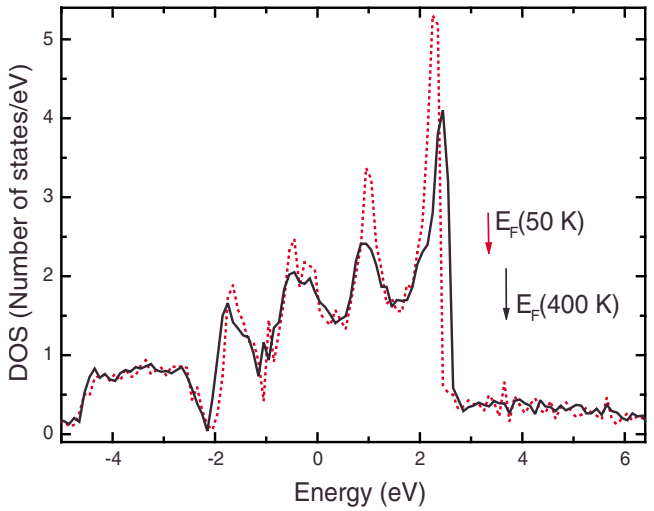

FIG. 5. (Color online) Electronic density of states of palladium hydride at two temperatures: 50 K (dotted/red) and 400 K (solid/black).

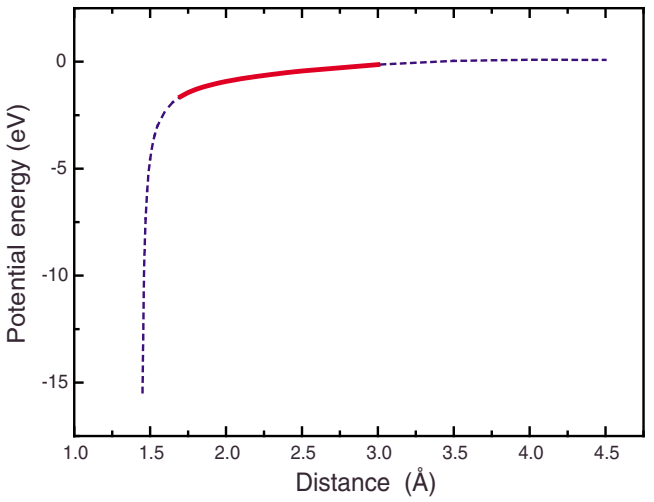

FIG. 6. (Color online) Potential energy of interaction between two hydrogen atoms calculated with the NRL-TB set of parameters; dashed (blue) line shows wide range of distances exceeding the range used for the TB fit shown by solid (red) line.

0.19 a.u.[27] The precise calculations of the mean-squared displacement should include the corrections due to the zero-point vibrations typical for the hydrogen atoms in the lattice of heavy metals.[28]

F. Electronic density of states

We have determined the electronic DOS and the position of the Fermi level for various temperatures in the range from 0 K up to 900 K. The density of states is found by counting the number of eigenvalues within a bin of 0.1 eV width over all k points included in the calculations. At zero temperature the DOS of palladium has a sharp maximum near the Fermi level which is approximately the energy where the d bands end. This sharp change in energy requires a higher number of k points for the molecular dynamics simulations to increase the precision in the calculations of forces. We determined that at least 108 k points were needed for the supercell of 64 palladium atoms to provide stability of the MD simulations. The DOS of palladium hydride (see Fig. 5) is changing relatively slowly near the Fermi level (which lies above the d bands) and the number of k points can be reduced to 32.

G. Vacancy formation energy

We have studied the nonstoichiometric compositions of the palladium hydride by applying the TBMD simulations to the palladium-hydrogen system with various concentrations of hydrogen. This study is aimed to understand the limit of solubility of hydrogen in palladium lattice. The problem of solubility requires knowledge on energies in both the solid phase of palladium-hydrogen system and the gaseous phase of hydrogen. The changes in the total energy on each side include the electronic energy of interatomic bonds dissociated and formed as well as the kinetic and potential energy of the movement of atoms.

Our method provides the model Hamiltonian of electronic system which describes with high accuracy the changes in energy of electronic states formed by bonding of atomic orbitals of atoms in all systems included into the model. The accuracy is achieved by fitting the NRL-TB to the LAPW energies calculated for a large number of structures. With this Hamiltonian we can accurately calculate the difference in the electronic energy between two atomic configurations with two different compositions and interatomic distances. The transferability of the NRL-TB method makes it possible to calculate the variations in the electronic energies for a large number of atomic compositions and a relatively wide range of interatomic distances. Although the range of atomic distances is substantially wide, it is limited by a functional form of the TB parameters used in the NRL-TB. In particular, the hopping parameters are approximated by Eq. (3) which includes the positive powers of the interatomic distances only. This functional form leads to the attractive interatomic potential for all distances including the short-range potential where the interaction should be repulsive. This limits our method to only be applied within a range of distances substantially longer than a distance comparable to a size of the hydrogen molecule where atoms are located near the repulsive range of the interatomic potential. Figure 6 illustrates the problem. The dashed line shows the potential energy of interaction between two hydrogen atoms which is calculated with the parameters obtained from the fit in the range shown by the solid line. The potential is attractive as expected in the fitting range. At short distance, the energy continues to decrease making the short-range part inapplicable.

Within the range of applicability, we still can obtain a valuable information about the relative changes in energy of various structures. We have calculated the energy of palladium hydride as a function of the hydrogen content. The energy change can be viewed as consisting of two contributions. One is due to the bonding between each hydrogen atom and its palladium neighbors. The lattice of hydrogen and palladium atoms already bonded vary its energy depending on the positions and distances. This second contribution

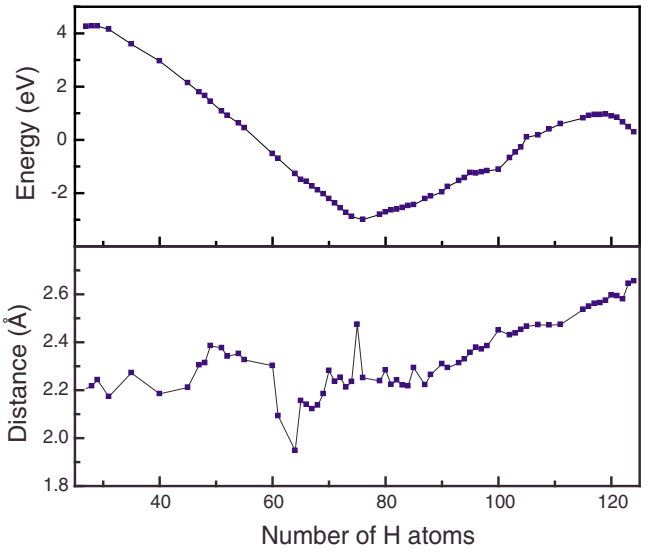

FIG. 7. (Color online) Energy formation and distance between nearest H atoms calculated for $Pd_{125}H_n$ supercell ($25 \leq n \leq 125$).

can be studied by the TBMD method since the distances between the atoms remain in the range where the TB Hamiltonian is applicable. We calculate the energies of these atomic configurations. We can compare these energies after subtracting the bonding energies. The variations in the energy provide the information which configurations are stable and energetically preferable provided that other contributions to the total energy are balanced including the bonding and kinetic energies of atoms.

We have calculated the energy of palladium hydride as a function of the hydrogen content. The calculations are based on the method similar to the vacancy formation energy calculations which we employed for vacancies and divacancies in palladium.[16] We calculated the energy of structures with compositions between palladium and stoichiometric palladium hydride, E_{PdH_x} for a supercell consisting of 125 Pd atoms and a varying number of H atoms, $n=125x(0.2 \leq x \leq 1)$, randomly removed from the stoichiometric palladium hydride. We also calculated the energy of stoichiometric palladium hydride, E_{PdH}, and the energy of fcc palladium structure, E_{Pd} with the same distance between palladium atoms as in palladium hydride. The latter is used as a reference point for the energy of palladium hydride. The difference between E_{PdH} and E_{Pd} divided by the number of hydrogen atoms gives us the bonding energy of each hydrogen atom in the palladium hydride. We subtract this energy multiplied by the number of hydrogen atoms in a specific PdH_x configuration to eliminate the bonding energy of hydrogen. In this approximation, the bonding energy changes linearly with the hydrogen content, x. The deviation from the linear trend is

$$\Delta E_{PdH_x} = E_{PdH_x} - E_{Pd} - x(E_{PdH} - E_{Pd}). \quad (6)$$

Figure 7(a) shows ΔE_{PdH_x} as a function of x. The minimum of the deviation is between 60% and 70% near the experimental limit of solubility reached experimentally. Although this minimum is not the minimum of the total energy, we can likely conclude that the hydrogen concentration in the range of 60–70 % is energetically preferable for the solid palladium hydride structures.

In all these structures, the distance between hydrogen atoms remains within the range of applicability of the TB Hamiltonian discussed above. This indicates that the positions of hydrogen atoms are primarily controlled by the interactions with the palladium neighbors and the direct hydrogen-hydrogen interactions do not play a significant role in configurations with the hydrogen content below $x=1$. Above we assumed that the bonding energy of hydrogen atoms is mostly determined by the nearest palladium neighbors of each hydrogen atom and we calculated the bonding energy from the energy of the stoichiometric structure. The weakness of the direct H-H interactions justifies our assumption. The dominating role of the hydrogen-palladium interaction is also compliant with our observations for the frequencies of optical and acoustic phonons which point to the softening of the potential seen by hydrogen near the stoichiometric composition while palladium lattice experiences relatively small changes. For a further study of hydrogen distribution, we have also determined the nearest H-H distance for each structure. We recorded the atomic positions and found the minimum distance between two hydrogen atoms for each MD step shown in Fig. 7(b). The distance between the nearest hydrogen atoms fluctuates but for virtually all configurations, it evidently remains above the limit of 2.1 Å given by the Switendick criterion.[29]

IV. SUMMARY

We have used the NRL-TB method to perform both static and dynamic calculations of various properties of PdH(D). This work capitalizes on the fact that the TBMD method substantially reduces the computational cost in comparison with first-principles methods which currently appear to be not practical for such massive calculations. The MD calculations exploited the computational speed of the TB method and made it possible to perform calculation of 250 atoms in the unit cell with 64 k points and for 3000 MD steps. Our runs used parallelization of the MD code for up to 32 nodes on an SGI Altix computer. A typical run took approximately 30 h. We expect that a similar calculation using one of the first-principles codes would be more than a factor of 10–100 times slower depending on using pseudopotential or all-electron method.

ACKNOWLEDGMENTS

We thank Joseph L. Feldman for helpful discussions. This work is supported by the U.S. Department of Energy Award No. DE-FG02-07ER46425.

APPENDIX

Tight-binding parameters for PdH, generated following the methods of Mehl and Papaconstantopoulos[14] and Bernstein *et al.*[30] On-site energies are generated from the densities of Pd and H atoms: $\rho_{\mathrm{Pd}}=\Sigma_{\mathrm{Pd}}\exp(-\lambda_{\mathrm{Pd}}^2 R)F(R)$, where $\lambda_{\mathrm{Pd}}=1.2880$ a.u.$^{-1/2}$ and $\rho_{\mathrm{H}}=\Sigma_{\mathrm{H}}\exp(-\lambda_{\mathrm{H}}^2 R)F(R)$, where $\lambda_{\mathrm{H}}=0.84159$ a.u.$^{-1/2}$. $F(R)$ is the cutoff function from Eq. (2) of Bernstein *et al.*,[30] with $R_c=16.5$ a.u. and $L_c=0.5$ a.u. All energies are in Rydberg and all distances in atomic unit.

Pd-Pd interactions

On-site parameters $h_l=a_l+b_l\rho_{\mathrm{Pd}}^{2/3}+c_l\rho_{\mathrm{Pd}}^{4/3}+d_l\rho_{\mathrm{Pd}}^2$

l	a_l	b_l	c_l	d_l
s	0.04807	27.738	−969.51	22847.
p	0.57335	24.921	−669.76	7360.9
d	0.04051	0.72555	3.4858	−86.808

Hopping terms $H_{ll'u}(R)=(e_{ll'u}+f_{ll'u}R+g_{ll'u}R^2)\exp(-q_{ll'u}^2 R)F(R)$

$H_{ll'u}$	$e_{ll'u}$	$f_{ll'u}$	$g_{ll'u}$	$q_{ll'u}$
$H_{ss\sigma}$	−6.3923	1.1511	−0.47063	1.0361
$H_{sp\sigma}$	1.2649	0.25963	0.03103	0.81918
$H_{pp\sigma}$	−10.362	−1.0017	0.92481	0.93593
$H_{pp\pi}$	3.5640	−1.8254	0.13354	0.85261
$H_{sd\sigma}$	0.71794	−0.91057	−0.07435	0.93272
$H_{pd\sigma}$	11.656	−3.2504	−0.06050	0.94161
$H_{pd\pi}$	−19.231	7.0242	0.25794	1.1206
$H_{dd\sigma}$	10.299	−3.4069	0.00721	1.0139
$H_{dd\pi}$	1.4904	−9.1084	3.8189	1.1964
$H_{dd\delta}$	−390.81	232.81	−26.964	1.4433

Overlap terms $S_{ll'u}(R)=(\bar{e}_{ll'u}+\bar{f}_{ll'u}R+\bar{g}_{ll'u}R^2)\exp(-\bar{q}_{ll'u}^2 R)F(R)$

$S_{ll'u}$	$\bar{e}_{ll'u}$	$\bar{f}_{ll'u}$	$\bar{g}_{ll'u}$	$\bar{q}_{ll'u}$
$S_{ss\sigma}$	3.0077	−0.15638	−0.02704	0.68759
$S_{sp\sigma}$	−2.1653	−0.53362	0.06923	0.84405
$S_{pp\sigma}$	−22.418	7.8234	−1.2656	0.98059
$S_{pp\pi}$	188.13	−73.633	8.0682	1.0704
$S_{sd\sigma}$	−0.22069	0.17646	0.04321	0.84791
$S_{pd\sigma}$	−2.1505	0.43175	−0.01089	0.68648
$S_{pd\pi}$	−10.577	0.88181	0.37926	0.96803
$S_{dd\sigma}$	583.28	126.21	33.309	1.4844
$S_{dd\pi}$	−1.1894	−0.10777	0.02561	0.79519
$S_{dd\delta}$	1.7408	0.14079	0.02149	0.98143

H-H interactions

On-site parameters $h_l=a_l+b_l\rho_{\mathrm{H}}^{2/3}+c_l\rho_{\mathrm{H}}^{4/3}+d_l\rho_{\mathrm{H}}^2$

l	a_l	b_l	c_l	d_l
s	0.24555	0.27111	0.01093	0.07728
p	1.2692	−0.08594	−0.21199	−0.27801

Hopping terms $H_{ll'u}(R)=(e_{ll'u}+f_{ll'u}R+g_{ll'u}R^2)\exp(-q^2_{ll'u}R)F(R)$

$H_{ll'u}$	$e_{ll'u}$	$f_{ll'u}$	$g_{ll'u}$	$q_{ll'u}$
$H_{ss\sigma}$	16.515	0.17840	0.18736	1.0675
$H_{sp\sigma}$	−0.13898	−0.03387	−0.00106	0.56659
$H_{pp\sigma}$	0.17997	0.05310	0.01802	0.61214
$H_{pp\pi}$	21.312	3.4509	0.41243	1.1765

Overlap terms $S_{ll'u}(R)=(\bar{e}_{ll'u}+\bar{f}_{ll'u}R+\bar{g}_{ll'u}R^2)\exp(-\bar{q}^2_{ll'u}R)F(R)$

$S_{ll'u}$	$\bar{e}_{ll'u}$	$\bar{f}_{ll'u}$	$\bar{g}_{ll'u}$	$\bar{q}_{ll'u}$
$S_{ss\sigma}$	39.931	1.8425	−2.3724	1.0823
$S_{sp\sigma}$	0.37803	−0.40186	−0.01243	0.94884
$S_{pp\sigma}$	3.7892	−0.09191	0.00270	0.75749
$S_{pp\pi}$	0.35224	0.02048	−0.01089	0.54363

Pd-H interactions

On-site parameters $h_{l(\mathrm{Pd})}=b_l\rho_{\mathrm{H}}^{2/3}+c_l\rho_{\mathrm{H}}^{4/3}+d_l\rho_{\mathrm{H}}^2$

l	b_l	c_l	d_l
s	0.02841	−0.02372	−0.07125
p	0.03492	0.00882	0.00954

On-site parameters $h_{l(\mathrm{H})}=b_l\rho_{\mathrm{Pd}}^{2/3}+c_l\rho_{\mathrm{Pd}}^{4/3}+d_l\rho_{\mathrm{Pd}}^2$

l	b_l	c_l	d_l
s	2.9322	60.098	1153.9
p	1.5965	38.358	1267.5

Hopping terms $H_{ll'u}(R)=(e_{ll'u}+f_{ll'u}R+g_{ll'u}R^2)\exp(-q^2_{ll'u}R)F(R)$

$H_{ll'u}$	$e_{ll'u}$	$f_{ll'u}$	$g_{ll'u}$	$q_{ll'u}$
$H_{ss\sigma}$	−0.45416	−0.05871	0.04298	0.76758
$H_{sp\sigma}$	0.17453	0.05522	0.01674	0.72297
$H_{pp\sigma}$	−2.1200	0.09348	0.05199	0.73834
$H_{pp\pi}$	0.00812	−0.01380	−0.00060	0.71359
$H_{ps\sigma}$	1.8691	0.30642	−0.14296	0.99247
$H_{ds\sigma}$	−1.6572	−0.49398	−0.08927	0.99691
$H_{dp\sigma}$	0.70937	0.18817	0.05284	1.0241
$H_{dp\pi}$	0.07305	0.03441	0.02136	0.92624

Overlap terms $S_{ll'u}(R)=(\bar{e}_{ll'u}+\bar{f}_{ll'u}R+\bar{g}_{ll'u}R^2)\exp(-\bar{q}^2_{ll'u}R)F(R)$

$S_{ll'u}$	$\bar{e}_{ll'u}$	$\bar{f}_{ll'u}$	$\bar{g}_{ll'u}$	$\bar{q}_{ll'u}$
$S_{ss\sigma}$	−1.8913	0.01111	0.08878	0.79915
$S_{sp\sigma}$	0.11866	−0.03077	−0.01818	0.72583
$S_{pp\sigma}$	0.30489	−0.21013	0.00020	0.74882
$S_{pp\pi}$	−0.28112	−0.06840	−0.01940	1.0883
$S_{ps\sigma}$	−1.0808	−2.3212	−0.68882	1.1572
$S_{ds\sigma}$	299.99	39.354	1.4383	1.6287
$S_{dp\sigma}$	−1.7937	0.92290	0.81594	1.0359
$S_{dp\pi}$	0.11598	1.1318	0.57892	1.2534

[1] T. Graham, Philos. Trans. R. Soc. London **156**, 399 (1866).
[2] F. A. Lewis, *The Palladium Hydrogen System* (Academic Press, London, New York, 1967).
[3] F. A. Lewis, Platinum Met. Rev. **26**, 20 (1982).
[4] E. Wicke and H. Brodowsky, in *Hydrogen in Metals*, edited by G. Alefeld and J. Volkl (Springer-Verlag, Berlin, 1978).
[5] T. B. Flanagan and W. A. Oates, Annu. Rev. Mater. Sci. **21**, 269 (1991).
[6] A. C. Switendick, Ber. Bunsenges. Phys. Chem. **76**, 535 (1972).
[7] D. A. Papaconstantopoulos and B. Klein, Phys. Rev. Lett. **35**, 110 (1975); D. A. Papaconstantopoulos, B. M. Klein, E. N. Economou, and L. L. Boyer, Phys. Rev. B **17**, 141 (1978).
[8] C. T. Chan and S. G. Louie, Phys. Rev. B **27**, 3325 (1983).
[9] J. K. Nørskov, Phys. Rev. B **26**, 2875 (1982).
[10] M. S. Daw and M. I. Baskes, Phys. Rev. B **29**, 6443 (1984).
[11] D. A. Papaconstantopoulos, B. M. Klein, J. S. Faulkner, and L. L. Boyer, Phys. Rev. B **18**, 2784 (1978).
[12] D. A. Papaconstantopoulos and M. J. Mehl, J. Phys.: Condens. Matter **15**, R413 (2003).
[13] J. C. Slater and G. F. Koster, Phys. Rev. **94**, 1498 (1954).
[14] M. J. Mehl and D. A. Papaconstantopoulos, Phys. Rev. B **54**, 4519 (1996).
[15] R. E. Cohen, M. J. Mehl, and D. A. Papaconstantopoulos, Phys. Rev. B **50**, 14694 (1994).
[16] A. Shabaev and D. A. Papaconstantopoulos, Phys. Rev. B **79**, 064107 (2009).
[17] P. Aben and W. G. Burgers, Trans. Faraday Soc. **58**, 1989 (1962).
[18] J. E. Schirber and B. Morosin, Phys. Rev. B **12**, 117 (1975).
[19] S. W. Wei and M. Y. Chou, Phys. Rev. Lett. **69**, 2799 (1992).
[20] A. P. Miiller and B. N. Brockhouse, Phys. Rev. Lett. **20**, 798 (1968).
[21] J. Rowe, J. Rush, H. Smith, M. Mostoller, and H. Flotow, Phys. Rev. Lett. **33**, 1297 (1974).
[22] B. M. Klein and R. E. Cohen, Phys. Rev. B **45**, 12405 (1992).
[23] D. K. Hsu and R. G. Leisure, Phys. Rev. B **20**, 1339 (1979).
[24] F. Kirchhoff, M. J. Mehl, N. I. Papanicolaou, D. A. Papaconstantopoulos, and F. S. Khan, Phys. Rev. B **63**, 195101 (2001).
[25] A. C. Bailey, N. Waterhouse, and B. Yates, J. Phys. C **2**, 769 (1969).
[26] L. M. Peng, G. Ren, S. L. Dudarev, and M. J. Whelan, Acta Crystallogr., Sect. A: Found. Crystallogr. **52**, 456 (1996).
[27] J. Worsham, M. Wilkinson, and C. Shull, J. Phys. Chem. Solids **3**, 303 (1957).
[28] A. F. Andreev, in *Quantum Theory of Solids*, edited by I. M. Lifshits (Mir, Moscow, 1982).
[29] A. C. Switendick, Z. Phys. Chem. **117**, 89 (1979).
[30] N. Bernstein, M. J. Mehl, D. A. Papaconstantopoulos, N. I. Papanicolaou, M. Z. Bazant, and E. Kaxiras, Phys. Rev. B **62**, 4477 (2000).